IAC-21-A6.5.3

Comparison of Relative Motion Control Algorithms for Point Capturing of Space Debris Object

Mahdi R. Akhloumadi[a]*, Danil Ivanov[b], Filipp Kozin[c]

[a] *Moscow Institute of Physics and Technology, Moscow Region, Russia,* akhloumadi@gmail.com
[b] *Space Systems Dynamics Department, Keldysh Institute of Applied Mathematics, RAS, Moscow, Russian Federation,* danilivanovs@gmail.com
[c] *Space Systems Dynamics Department, Keldysh Institute of Applied Mathematics, RAS, Moscow, Russian Federation,* filipp.kozin@gmail.com
* Corresponding Author

Abstract

A small satellite equipped with thrusters providing continuous limited thrust for translational control is considered in the paper. The angular motion of the satellite is controlled by onboard reaction-wheels. The position of the capturing point of the space debris object and the position of the capturing system in the satellite body frame are assumed to be specified. One of the proposed control algorithm is constructed based on State-Dependent Riccati Equation to provide the required relative attitude and position of these two points for the capturing. The control algorithm requires linearization of nonlinear motion equations in the vicinity of the current state vector. The optimal control coefficients are determined by solving the Riccati equation at each time step. Another approach is to use artificial potentials to develop a control algorithm for achieving capturing conditions. Attractive and repulsive potentials are virtually placed in the space debris centre of mass, and a conical selective potential is in the vicinity of capturing point. The satellite reaches the required relative distance and capture the object in case the point of the space debris object and the position of the capturing system are close to each other. These two control algorithms performance is studied using numerical simulation with defined parameters of supposed active space debris removal mission. The results of the algorithms application are compared, their main features and shortcomings are analysed.

Keywords: active space debris removal, motion control, virtual potentials, SDRE

1. Introduction

Space debris removal problem is one of the most complex and urgent task for space community. A set of missions are already tested a set of approaches for debris removal [1–5]. Active removal of inactive spacecrafts and rocket stages often involves the use of special small satellites that can attach themselves on the space debris object or capture it with a manipulator [6], net [7,8] or harpoon with tether [9,10], and change its orbit using the on-board motion control system. Active debris removal implies autonomous relative motion control in order to achieve relative state vector required for capturing. Onboard propulsion is often considered for the translational motion control and reaction wheels are for the attitude maneuvers.

The problem of relative translational and attitude motion control is well studied and a big variety of control approaches is developed. For example, sliding control-based algorithms [11,12] are developed for the relative orbit-attitude tracking problem, for the rendezvous problem the swarm particle optimization algorithm is applied for the required trajectories generation [13], for the docking stage with non-cooperative object the majority of the proposed control algorithms are fuel-optimal or time-optimal [14–18]. Therefore, the optimal algorithms for calculating trajectories are often replaced by computationally simpler and faster non-optimal ones [19,20], however their performance are strongly depend on initial conditions at the docking stage. As a compromise between two approaches a feedback control law developed for minimization of some defined cost-function can be applied to the problem. A linear quadratic regulator (LQR) is well-known example of such an algorithm, though the relative motion equations are highly non-linear. To overcome this inconsistency the motion equations are linearized in the vicinity of the current state vector and LQR-like State-Dependent Riccati Equation-based (SDRE) control algorithm is applied [21–23]. In [24,25] a comparative study between SDRE and LQR is presented, and SDRE showed its advantages considering fuel consumption, rendezvous time and trajectory accuracy. The SDRE-based algorithms are used to address various problems such as the position and attitude control of a single spacecraft [26] or relative motion control in satellite formation flying [25]. For the problem of space debris

object capturing the kinematic coupling effect must be taken into account when the relative motion of not centers of mass of two bodies but motion between two defined body-fixed points is considered as in [27]. The paper [28] studies the application of the SDRE-based control for this type of relative motion equations. In paper [29] the influence of the control system parameters on the performance of the SDRE-based control algorithm on the relative motion during the capturing taking into account reaction wheels saturation and thrusters misalignment is studied.

The presented paper devoted to comparison of two different control approaches for capturing the tumbling space debris at the defined point. Performance of the SDRE-based control algorithm and virtual potentials approach are studied at the same conditions and with the same parameters of the satellite and the satellite system. Such a study allows to choose the most appropriate algorithm depending on requirements of the space debris removal mission.

2. Problem Statement

Consider a tumbling space debris object and a satellite capable to capture this object by some of the capturing system such as robotic manipulator, magnetic gripper, harpoon etc. The satellite initially is in a certain vicinity of several meters near the debris object. In order to capture the object the satellite should be inside the defined area relative to the capturing point on the object surface and the satellite capturing system should be directed to the capturing point with required accuracy. The main purpose of the motion control system is to provide such a translational and attitude motion of the satellite that will result in satisfying the capturing conditions concerning the relative center of mass position and relative attitude. It is assumed that the satellite is equipped with onboard propulsion system able to provide continuous thrust and with reaction wheels for attitude control.

The purpose of the paper is to develop motion control algorithms for capturing maneuver in a close range and compare its performance in required characteristic velocity and maneuver time. The body-fixed reference frames of the tumbling space debris object and active satellite are presented in Fig. 1.
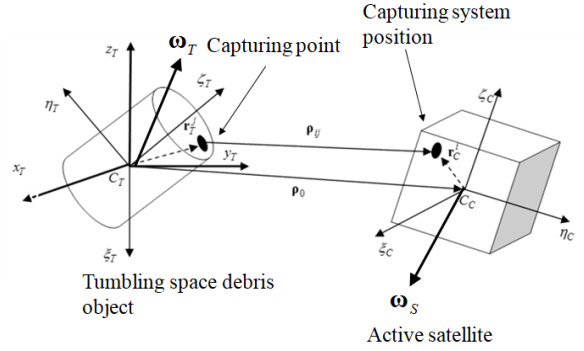
Fig. 1. Reference frames of chaser satellite and target object

3.1 Relative rotational and translational equations of motion

In this section the equations of rotational and translational motion are derived. A relative vector is formed using relative velocity and distance between two specified points on the space debris and satellite. This relative vector between arbitrary points couples the rotational and translational motion of two objects. In order to represent the dynamical equations of motion in terms of relative vector of distance and velocity between these two points, it is required to use relative translational equations of centres of mass and the relative rotational equation of two rigid object.

In order to express relative rotational motion and corresponding equations, angular momentum equations of (1.1) and (1.2):

$$\left(\frac{d\mathbf{H}_S}{dt}\right)_I = \left(\frac{d\mathbf{H}_S}{dt}\right)_S - \boldsymbol{\omega}_S \times \mathbf{H}_S = \mathbf{N}_S + \mathbf{T}_S \quad (1.1)$$

$$\left(\frac{d^I\mathbf{H}_D}{dt}\right) = \left(\frac{d^D\mathbf{H}_D^D}{dt}\right) - \boldsymbol{\omega}_D^D \times \mathbf{H}_D^D = \mathbf{N}_D^D \quad (1.2)$$

In these equations (1.1) (1.2) $\mathbf{H}_C, \mathbf{H}_D$ are the angular momentum of chaser and the target. The subscript placeholder for I, T denotes the system of the coordinates where differentiating. $\mathbf{N}_C, \mathbf{N}_D$ stands for external disturbing torques and $\mathbf{T}_C$ is control. at the same time can introduce relative angular velocity as:

$$\boldsymbol{\omega} = \boldsymbol{\omega}_S - \boldsymbol{\omega}_D \quad (1.3)$$

Where $\boldsymbol{\omega}_S, \boldsymbol{\omega}_D$ are angular velocities of the spacecraft and the debris. Differentiating (1.3) in inertial frame and expressing in the target reference frame leads to relative kinematics of two space object as

$$\left(\frac{d^I\boldsymbol{\omega}}{dt}\right)^D = \mathbf{D}_S^D \left(\frac{d^I\boldsymbol{\omega}_S}{dt}\right)^S - \left(\frac{d^I\boldsymbol{\omega}_D}{dt}\right)^D, \quad (1.4)$$

where $\mathbf{D}_S^T$ is the transfer matrix from spacecraft to the target. Notting that:

$$\mathbf{H}_S = \mathbf{I}_S \boldsymbol{\omega}_S + \mathbf{h}_{WS}, \ \mathbf{H}_D = \mathbf{I}_D \boldsymbol{\omega}_D \qquad (1.5)$$

Then the dynamical equations of relative rotational motion can be derived in debris reference frame:

$$\mathbf{I}_D \dot{\boldsymbol{\omega}}^D = \boldsymbol{\omega}^D \times \mathbf{I}_D \boldsymbol{\omega}_D^D +$$
$$+ \mathbf{I}_D \mathbf{D} \mathbf{I}_S^{-1} \left(\mathbf{T}_S^S - \mathbf{D}^{-1} \left(\boldsymbol{\omega}^D + \boldsymbol{\omega}_D^D \right) \times \mathbf{I}_S \mathbf{D}^{-1} \left(\boldsymbol{\omega}^D + \boldsymbol{\omega}_D^D \right) \right)$$
$$- \boldsymbol{\omega}_D \times \mathbf{I}_D \boldsymbol{\omega}_D.$$
$$(1.6)$$

At the same time relative translational equations of motion which are called Clohessy-Wiltshire for the centres of mass of two objects are as follow:

$$\ddot{x} = n^2 x + 2n\dot{y} + a_x$$
$$\ddot{y} = -2n\dot{x} + a_y \qquad (1.7)$$
$$\ddot{z} = -n^2 z + a_z$$

where $\boldsymbol{\rho}_0 = [x; y; z]^T$ is radius-vector of chaser center of mass in LHLV reference frame with target in the origin C_T (Fig. 1); $\mathbf{a} = \begin{bmatrix} a_x & a_y & a_z \end{bmatrix}^T$ is the control acceleration, which is produced by thrusters; n is the orbital angular velocity of the target.

Now consider that two points are fixed on the spacecraft and space debris and are expressed in the body frames of this rigid bodies as P_S, P_D and the corresponding radius vectors from the centres of mass are $\mathbf{r}_S, \mathbf{r}_D$. The relative vector for capturing can be expressed as the sum of these two vectors

$$\mathbf{e}^D = \mathbf{D}_S^D \mathbf{e}_S^S + \mathbf{e}_D^D, \qquad (1.8)$$

where $\mathbf{e}_S, \mathbf{e}_D$ are the unit vectors from the center of mass of the corresponding object to these points. Taking derivative from (1.8) gives:

$$\left(\frac{d\mathbf{e}}{dt} \right)^D = \boldsymbol{\omega}^\times \mathbf{D}_S^D \mathbf{e}_S^S = \boldsymbol{\omega}^\times \mathbf{D}_D^S \mathbf{e}_S^S$$
$$= \boldsymbol{\omega}^\times \mathbf{D}_D^S (\mathbf{e}^D - \mathbf{e}_D^D) \qquad (1.9)$$

Where $\boldsymbol{\omega}^\times$ is the skew-symmetric matrix of vector $\boldsymbol{\omega}$. The second derivative of (1.8) is:

$$\left(\frac{d^2\mathbf{e}}{dt^2} \right)^T = \left(\dot{\boldsymbol{\omega}}^\times + \boldsymbol{\omega}^\times \boldsymbol{\omega}^\times \right)(\mathbf{e}^T - \mathbf{e}_T^T) \qquad (1.10)$$

(1.6) Can be simplified to

$$\dot{\boldsymbol{\omega}}^D = \mathbf{G} + \mathbf{D}\mathbf{I}_S^{-1}\mathbf{T}_S^S$$
$$\mathbf{G} = -\mathbf{D}\mathbf{I}_S^{-1} \left(\mathbf{D}^{-1} \left(\boldsymbol{\omega}^D + \boldsymbol{\omega}_D^D \right) \times \mathbf{I}_S \mathbf{D}^{-1} \left(\boldsymbol{\omega}^D + \boldsymbol{\omega}_D^D \right) \right)(1.11)$$
$$- \mathbf{I}_D^{-1} \left(\boldsymbol{\omega}_D \times \mathbf{I}_D \boldsymbol{\omega}_D \right) + \boldsymbol{\omega}^D \times \boldsymbol{\omega}_D^D$$

Substituting $\dot{\boldsymbol{\omega}}^\times$ from equation (1.6)

$$\frac{d^2\mathbf{e}}{dt^2} = \left((\mathbf{G})^\times + \boldsymbol{\omega}^\times \boldsymbol{\omega}^\times \right)(\mathbf{e} - \mathbf{e}_D) - (\mathbf{e} - \mathbf{e}_D)^\times \mathbf{D}\mathbf{I}_S^{-1}\mathbf{T}_S^S \ (1.12)$$

This equation is the nonlinear dynamical equation of this relative vector $\mathbf{e}$ with states and control.

3. Control Algorithms

3.1 SDRE-based control

The nonlinear dynamical system is considered as
$$\dot{\mathbf{x}} = \mathbf{f}(\mathbf{x}(t)) + \mathbf{g}(\mathbf{x}(t), \mathbf{u}(t)) \qquad (1.13)$$

Here state vector is shown as $\mathbf{x}(t) \in \mathbb{R}^n$ and the control vector as $\mathbf{u}(t) \in \mathbb{R}^m$, $\mathbf{f}, \mathbf{g}$ are nonlinear smooth functions; SDRE control algorithm can be generated for the nonlinear system (1.13) using the functional (1.14) to be minimized:

$$J = \frac{1}{2} \int_0^{t_f} \left[\mathbf{x}(t)^T \mathbf{Q} \mathbf{x}(t) + \mathbf{u}(t)^T \mathbf{R} \mathbf{u}(t) \right] dt \qquad (1.14)$$

Where $\mathbf{Q}, \mathbf{R}$ are positive definite weighting matrices. In (1.14) finite horizon time t_f is considered. Here the point $\mathbf{x} = 0$ is assumed to be equilibrium state of the system. SDRE method requires the linearization of the equation of motion in a neighbourhood of the equilibrium. The optimal coefficients of the regulator are calculated as a result of solving Riccati equation at each time step. In this paper $\mathbf{Q}, \mathbf{R}$ are considered as constant matrices. Next step is to linearize the nonlinear system. The linearization of dynamical system leads to:

$$\dot{\mathbf{x}} = \mathbf{A}(\mathbf{x})\mathbf{x} + \mathbf{B}(\mathbf{x})\mathbf{u} \qquad (1.15)$$

where $\mathbf{A}(\mathbf{x})$ is the dynamic matrix or state dependent coefficient matrix and $\mathbf{B}(\mathbf{x})$ is the nonlinear control matrix. analogical to linear quadratic regulator for nonlinear quadratic regulator a corresponding algebraic Riccati equation can be derived. Setting Hamilton function and applying the maximum principle of Pontryagin [31], and taking to account the necessary conditions for optimality leads to the optimal control law as:

$$\mathbf{u}(\mathbf{x}) = \mathbf{R}^{-1}\mathbf{B}^T(\mathbf{x})\mathbf{P}(\mathbf{x})\mathbf{X} \qquad (1.16)$$

The control function (1.16) is similar to linear quadratic regulator, but unlike LQR here the coefficients are implicit functions of state vector. The matrix $\mathbf{P}(\mathbf{x})$ is unique, symmetric and positive-definite and can be obtained by solving algebraic Riccati equation:

$$\begin{aligned} &\mathbf{P}(\mathbf{x})\mathbf{A}(\mathbf{x}) + \mathbf{A}^T(\mathbf{x})\mathbf{P}(\mathbf{x}) - \\ &- \mathbf{P}(\mathbf{x})\mathbf{B}(\mathbf{x})\mathbf{R}^{-1}(\mathbf{x})\mathbf{B}^T(\mathbf{x})\mathbf{P}(\mathbf{x}) + \mathbf{Q}(\mathbf{x}) = 0 \end{aligned} \quad (1.17)$$

After substituting this semi-optimal control law the closed loop system will look :

$$\dot{\mathbf{x}} = \left(\mathbf{A} - \mathbf{B}(\mathbf{x})\mathbf{R}^{-1}\mathbf{B}^T(\mathbf{x})\mathbf{P}(\mathbf{x})\right)\mathbf{x} \quad (1.18)$$

For the debris removal the dynamical equations (1.12) can be linearized with respect to $\mathbf{e}$ and $\dot{\mathbf{e}}$. state dependant factorizing of the equation system (1.12) will lead to:

$$\begin{aligned} &\begin{bmatrix} 0 & \mathbf{eye} \\ \left((\mathbf{ROD})^\times + \boldsymbol{\omega}^\times \boldsymbol{\omega}^\times\right) & 0 \end{bmatrix}_{6\times6} \begin{bmatrix} \mathbf{e} \\ \dot{\mathbf{e}} \end{bmatrix}_{6\times1} \\ &- \begin{bmatrix} 0 \\ (\mathbf{e} - \mathbf{e}_D)^\times \mathbf{DI}_S^{-1} \end{bmatrix}_{6\times3} \left[\mathbf{T}_S^S\right]_{3\times1} \end{aligned} \quad (1.19)$$

3.2 Virtual potentials approach

The second approach to the berthing process is to use virtual attractive and repulsive potential functions V_a, V_r. If these potential functions as (1.20) are added together, then it will be possible to achieve an equilibrium point in a desired distance between two centres. This equilibrium is the distance where the virtual net force is equal to zero, in the other words the potential functions compensate each other. The geometrical coefficient C_a, C_r, l_a, l_r are the geometrical coefficients of the poles and they determine the equilibrium position.

$$\begin{aligned} V_a &= -C_a e^{\frac{-r}{l_a}} \\ V_r &= C_r e^{\frac{-r}{l_r}} \\ V &= -C_a e^{\frac{-r}{la}} + C_r e^{\frac{-r}{lr}} = V_a + V_r \end{aligned} \quad (1.20)$$

The force produced by the potential function is :

$$-\nabla V = F \quad (1.21)$$

The components of the virtual force in orbital system are:

$$\begin{aligned} F_x &= \left(\frac{-C_a}{l_a} e^{\frac{-r}{l_a}} + \frac{C_r}{l_r} e^{\frac{r}{l_r}}\right)\frac{x}{r} = \left(\frac{V_a}{l_a} + \frac{V_r}{l_r}\right)\frac{x}{r}, \\ F_y &= \left(\frac{-C_a}{l_a} e^{\frac{-r}{l_a}} + \frac{C_r}{l_r} e^{\frac{r}{l_r}}\right)\frac{y}{r} = \left(\frac{V_a}{l_a} + \frac{V_r}{l_r}\right)\frac{y}{r}, \quad (1.22) \\ F_z &= \left(\frac{-C_a}{l_a} e^{\frac{-r}{l_a}} + \frac{C_r}{l_r} e^{\frac{r}{l_r}}\right)\frac{z}{r} = \left(\frac{V_a}{l_a} + \frac{V_r}{l_r}\right)\frac{z}{r}. \end{aligned}$$

Then by adding these virtual control forces to the right part of Clohessy-Wiltshire equation the relative motion can be controlled.

$$\begin{aligned} \ddot{x} &= n^2 x + 2n\dot{y} + \frac{\partial V}{\partial x} \\ \ddot{y} &= -2n\dot{x} + \frac{\partial V}{\partial y} \\ \ddot{z} &= -n^2 z + \frac{\partial V}{\partial z} \end{aligned} \quad (1.23)$$

In order to achieve a stable equilibrium point, some virtual friction will be added which leads to a semi-elliptical rotational movements around the target on the desired distance from the debris.

$$\begin{aligned} \ddot{x} &= n^2 x + 2n\dot{y} + \left(\frac{-C_a}{l_a} e^{\frac{-r}{l_a}} + \frac{C_r}{l_r} e^{\frac{r}{l_r}}\right)\frac{x}{r} + f_r e_r \frac{x}{|\mathbf{r}|} - \\ &\quad - f_r \left(V_{\tau x} - V_{\tau xd}\right), \\ \ddot{y} &= -2n\dot{x} + \left(\frac{-C_a}{l_a} e^{\frac{-r}{l_a}} + \frac{C_r}{l_r} e^{\frac{r}{l_r}}\right)\frac{y}{r} + f_r e_r \frac{y}{|\mathbf{r}|} - \\ &\quad - f_r \left(V_{\tau y} - V_{\tau yd}\right), \quad (1.24) \\ \ddot{z} &= -n^2 z + \left(\frac{-C_a}{l_a} e^{\frac{-r}{l_a}} + \frac{C_r}{l_r} e^{\frac{r}{l_r}}\right)\frac{z}{r} + f_r e_r \frac{z}{|\mathbf{r}|} - \\ &\quad - f_r \left(V_{\tau z} - V_{\tau xz}\right), \end{aligned}$$

where

$$\begin{aligned} e_r &= \mathbf{r}.\dot{\mathbf{r}}, \\ \mathbf{V}_\tau &= \dot{\mathbf{r}} - e_r \frac{\mathbf{r}}{|\mathbf{r}|}, \quad (1.25) \\ \mathbf{V}_\tau &= \alpha \frac{\mathbf{V}_\tau}{|V_\tau|}. \end{aligned}$$

And α is a control design coefficient. Using this algorithm it is possible to achieve an equilibrium distance around the target. The advantage of this

algorithm is that by changing the power coefficients C_a, C_r of the fields, it becomes possible to move toward the debris target when the proper time for capturing comes.

4. Algorithms comparison

Here the results of mathematical and computational modelling are presented. The rendezvous and capturing problem is solved using both algorithms. The same initial conditions for both simulations are as follow:

Table 1. Initial conditions

Initial conditions parameters	
P_S, P_D	[1,1,1] m
$\boldsymbol{\omega}_D^D(t_0)$	[0.2,0.4,0] rad/s
$\boldsymbol{\omega}_S^S(t_0)$	[0.02,0,0.08] rad/s
$\mathbf{q}_D(t_0)$	[0,0,1,0]
$\mathbf{q}_S(t_0)$	[0.59,0.2,0.6,0.5]
x_0	[5,5,5] m
$\dot{x}_0$	[1,2,3] m/s

For the simulation the following moment of inertia for the objects are considered:

$$\mathbf{I}_S = \begin{bmatrix} 2 & 0 & 0 \\ 0 & 3 & 0 \\ 0 & 0 & 4 \end{bmatrix} \text{kg}\cdot\text{m}^2,$$

$$\mathbf{I}_D = \begin{bmatrix} 1 & 0 & 0 \\ 0 & 1.4 & 0 \\ 0 & 0 & 1 \end{bmatrix} \text{kg}\cdot\text{m}^2. \quad (1.26)$$

For the SDRE algorithm the following weighting matrices for the translational motion control (1.27) and rotational (1.28) are used:

$$\mathbf{Q}_{attitude} = \mathbf{I}_6,$$
$$\mathbf{R}_{arrirude} = 10^{-3}\mathbf{I}_3, \quad (1.27)$$
$$\mathbf{Q}_{translation} = 1\mathbf{I}_6,$$
$$\mathbf{R}_{translation} = 10\mathbf{I}_3. \quad (1.28)$$

For the virtual potential method when the desired equilibrium distance is not reached yet, the geometrical and power C_a, C_r and friction f_r coefficient are suggested:

$$l_a, = 5, \; l_r = 2.755$$
$$C_a = 5, \; C_r = 4.5 \quad (1.29)$$
$$f_r = 1,$$

When the satellite is in the equilibrium distance and berthing opportunity shows up the coefficients change to the followings:

$$l_a, = 5, \; l_r = 2.755$$
$$C_a = 12, \; C_r = 1 \quad (1.30)$$
$$f_r = 0,$$

Fig. 2 and 3 show tracking error of the direction alignment of the berthing arm on spacecraft e_S and capturing point on the debris. When the capturing arm is directed towards the berthing vector, and the distance is reached to a desirable value, it is possible to accomplish the capturing Fig. 2 and 3 show the error of vectors e_S and $\dot{e}_S$ from the desired values. The SDRE algorithm provides a smooth convergence.
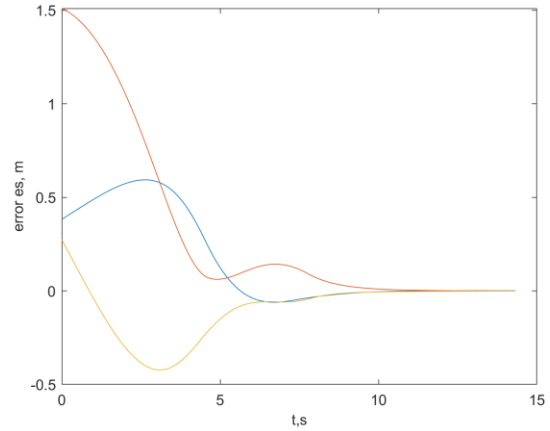
Fig. 2. Error of berthing vector on spacecraft
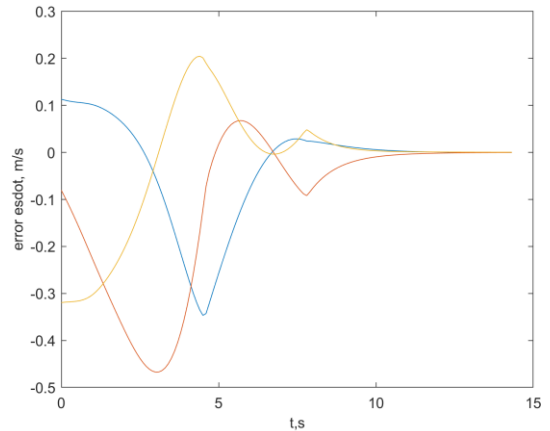
Fig.3. Error of berthing vector velocity on spacecraft

Animation which shows the relative trajectory is illustrated in Fig. 4. In a straight forward manner satellites goes to capture the debris.

IAC-21- A6.5.3
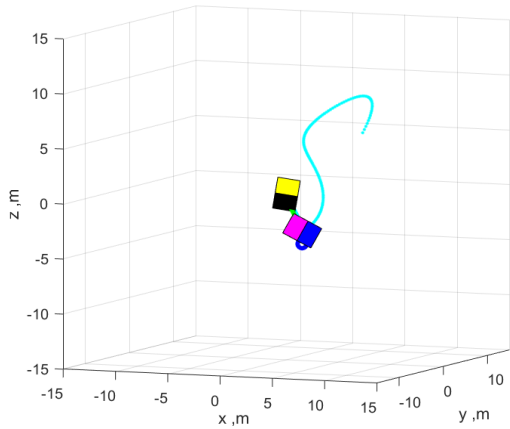
Fig. 4. Trajectory generated by SDRE

The translational force and rotational control torque are shown in Fig. 5-6. It is clear that to hold the direction and minimize distance for berthing constantly required to produce some control. Control magnitude is constraint due to limitation of controllers.
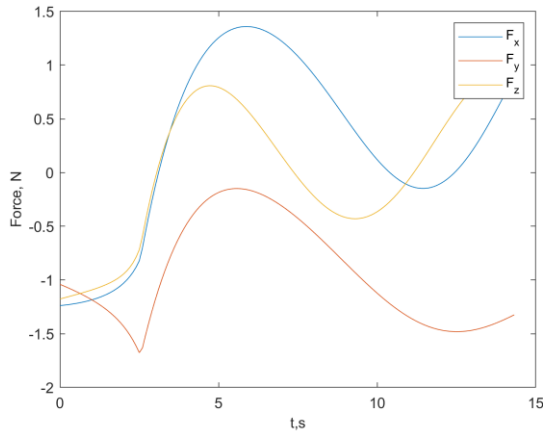
Fig. 5. Control force components
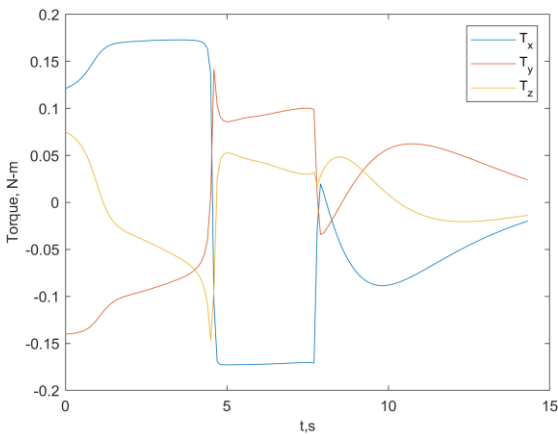
Fig. 6. Control torque on rotational motion

As mentioned with the same initial condition the problem simulated using the virtual repulsive and attractive potential method. Fig. 7-8 show the error of vectors e_s and $\dot{e}_s$ from the desired values. The virtual potential method provides a smooth convergence as well. The converging time for rendezvous vector alignment approximately is two times more than SDRE algorithm.
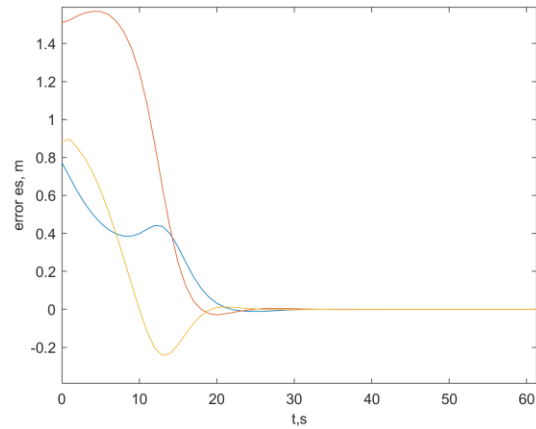
Fig. 7. Error of capturing vector on spacecraft
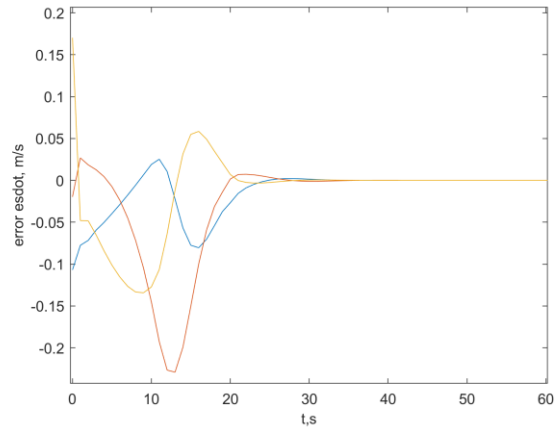
Fig. 8. Error of the capturing vector velocity on spacecraft

Animation demonstrating relative trajectory under virtual potentials is illustrated in Fig. 9. The satellite arrives to the desired equilibrium radius and by help of virtual friction rotates on the surface of an ellipsoid around the target until the time when the capturing conical window shows up. In this moment the attractive potential increases and satellites rush directly into the capturing sector. Here two possible cases happen. Either satellite can accomplish capturing on the available time successfully, or the sector closes and the satellites must retreat back to ellipsoid and wait for the sector to open up again and repeat the berthing process. Fig. 10 shows this event when first attempts are unsuccessful and then

satellite can finally accomplish capturing. For this case the angular velocity of the target is increased to [0.2,0.4,0.1] rad/s otherwise it could capture on the first attempt as Fig. 11.
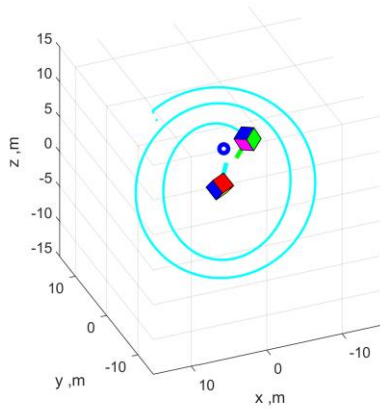
Fig. 9. Trajectory generated by virtual potentials
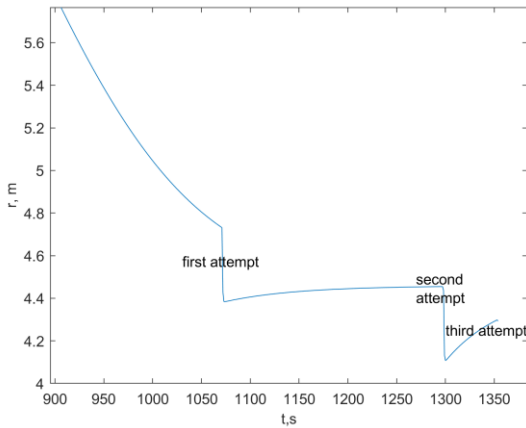
Fig. 10. Relative distance for the case of two unsuccessful attempts and third successful attempt for the docking
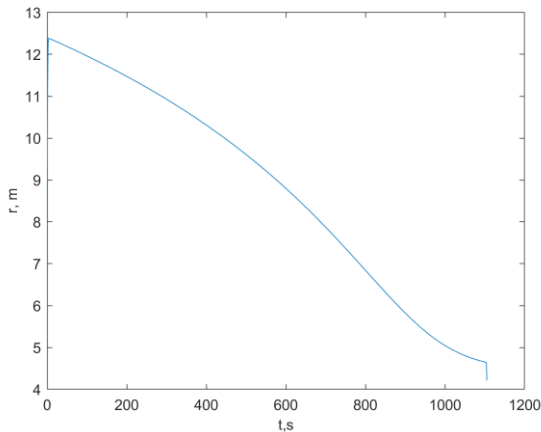
Fig. 11. First successful attempt

The translational force and rotational control torque are shown Fig. 12-13. In **Error! Reference source not found.** the near zero horizontal part of the graph shows the virtual friction and impulsive forces are the virtual potentials at approaching phase and capturing moment.
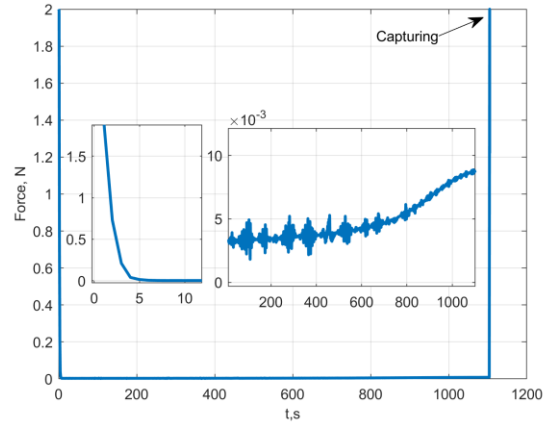
Fig. 12. Control force on translational motion virtual potentials
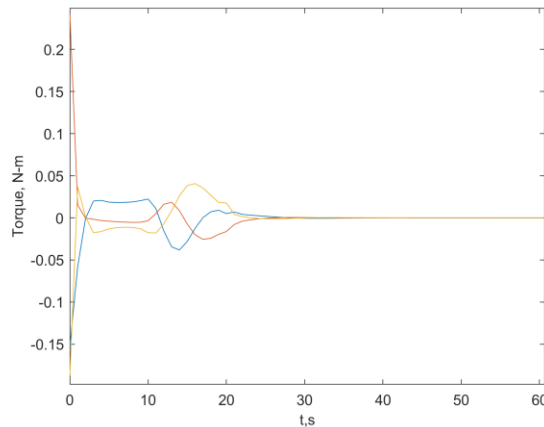
Fig. 13. Control torque on rotational motion virtual potentials

Another numerical study conducted in the following manner. Initial magnitude of angular velocity of the target is fixed and some sets of random points were taken, as a result the ΔV and capturing time is obtained. This comparative study is applied for both SDRE and potential methods. Fig. 14 demonstrate required ΔV for 7 sets of points with the fixed magnitude of angular velocity. Fig. 15 shows the rendezvous time for the same simulation. It is obvious that the more the angular velocity, the more the ΔV and rendezvous time.
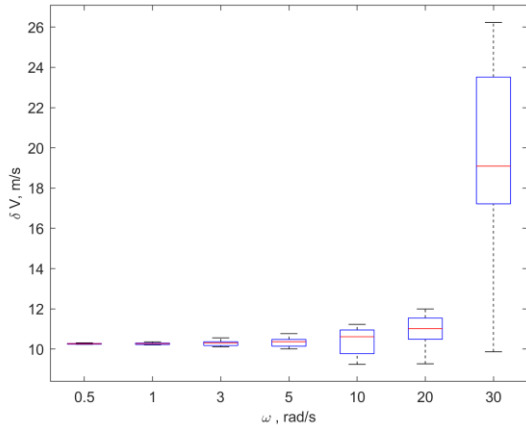
Fig. 14. Required Delta-V with respect to initial angular velocity of the debris for SDRE algorithm

Fig. 15. Capturing time with respect to initial angular velocity of the debris for SDRE algorithm

Fig. 16-17 the capturing time and the required ΔV is presented for the case of virtual potentials application. The capturing time is considerably more than the time required in case of SDRE-based control.
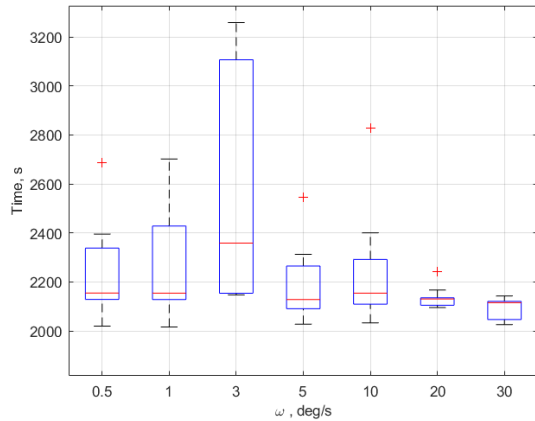
Fig. 16. Capturing time using virtual potential approach

Fig. 17. Delta-V with respect to trust value constraint for virtual potentials-based algorithm

The other comparative numerical study conducted by choosing some maximum values on thrust force as constraint, and at the same time choosing some sets of points with different initial distances and different debris angular velocity. Using this method shows the probability of a successful rendezvous and the time and corresponding fuel consumption which is required. Fig. 18-19 show that the higher the constraint value, the less ΔV and the less the rendezvous time for the SDRE algorithm is needed. Decreasing the constraint reduces the probability of successful work of algorithm.
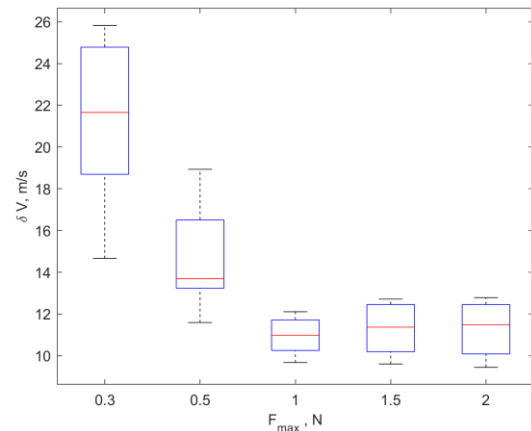
Fig. 18. ΔV with respect to trust value constraint for SDRE algorithm
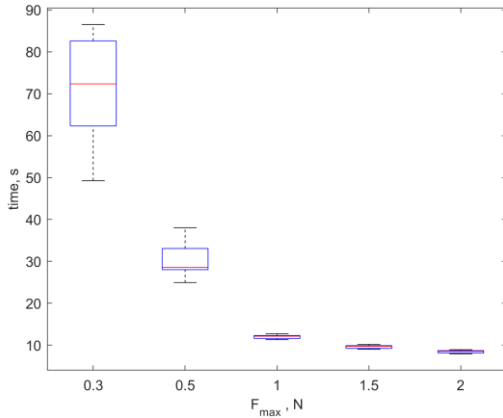
Fig. 19. Capturing time with respect to trust value constraint for SDRE algorithm

The capturing time depends on the desired precision as a predefined mission requirement. For this end some parameter is defined as terminal parameter which represents the accuracy of capturing. Fig. 20-21 show the ΔV and time for several terminal parameters for SDRE algorithm. The higher accuracy can be achieved at the cost of higher ΔV and rendezvous time.
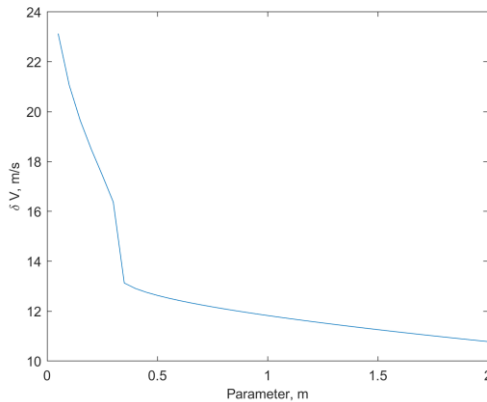
Fig. 20. Required Delta-V with respect to the terminal parameter for SDRE algorithm
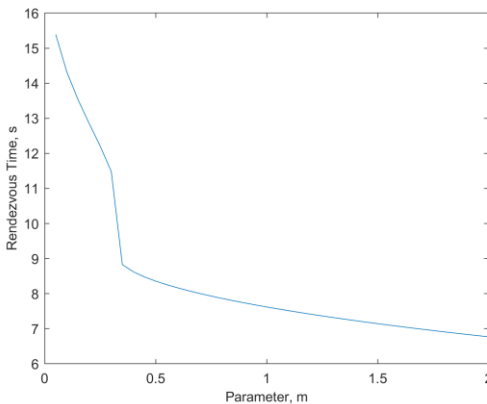
Fig. 21. Capturing time with respect to the terminal parameter for SDRE algorithm

The results for the case of virtual potential-based control algorithm is presented in Fig. 22-23. In case of low available thrust the vitual potential-based control failed to capture during the 10000 s. The higher the maximum thrust the faster the maneuver and it requires less ΔV.
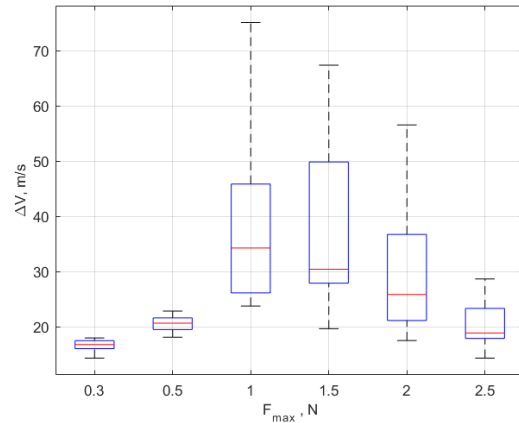
Fig. 22. Rendezvous time with respect to trust value constraint for SDRE algorithm
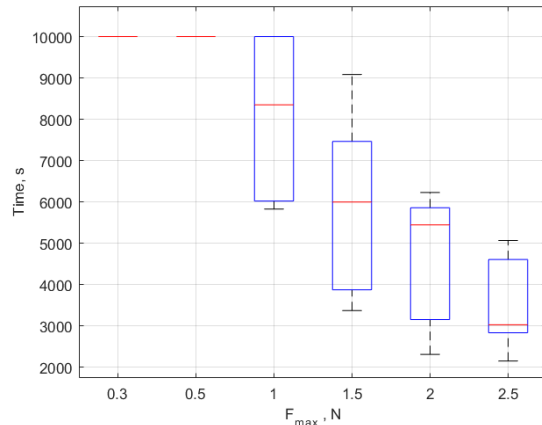
Fig. 23. Capturing time with respect to trust value constraint for SDRE algorithm

5. Conclusions

Two control approaches for active debris removal during the capturing stage is proposed in the work and their performance is compared under the same conditions. It has been shown that the SDRE-based control show faster convergence compared to algorithm using virtual potential functions. However, the required ΔV for the docking manoeuvre is more for the SDRE-based control. The advantage of the virtual potential-based algorithm is that along with saving fuel at cost of time it provides the collision avoidance in case of inappropriate relative position during the docking. Though at high space debris angular velocity the capturing could be not possible using this control

approach. One of the proposed algorithms could be implemented on-board depending on the space debris mission requirement concerning the constrains on the capturing manoeuver time and fuel limitation. Also the space debris angular velocity strongly affect the control algorithm performance.

Acknowledgements

References

1. Aglietti, G.S.; Taylor, B.; Fellowes, S.; Salmon, T.; Retat, I.; Hall, A.; Chabot, T.; Pisseloup, A.; Cox, C.; Zarkesh, A.; et al. The active space debris removal mission RemoveDebris. Part 2: In orbit operations. *Acta Astronaut.* **2020**, *168*, 310–322, doi:10.1016/j.actaastro.2019.09.001.
2. Hakima, H.; Bazzocchi, M.C.F.; Emami, M.R. A deorbiter CubeSat for active orbital debris removal. *Adv. Sp. Res.* **2018**, *61*, 2377–2392, doi:10.1016/j.asr.2018.02.021.
3. Shan, M.; Guo, J.; Gill, E. Review and comparison of active space debris capturing and removal methods. *Prog. Aerosp. Sci.* **2016**, *80*, 18–32, doi:10.1016/J.PAEROSCI.2015.11.001.
4. Bonnal, C.; Ruault, J.M.; Desjean, M.C. Active debris removal: Recent progress and current trends. *Acta Astronaut.* 2013, *85*, 51–60.
5. Mark, C.P.; Kamath, S. Review of Active Space Debris Removal Methods. *Space Policy* 2019, *47*, 194–206.
6. Felicetti, L.; Gasbarri, P.; Pisculli, A.; Sabatini, M.; Palmerini, G.B. Design of robotic manipulators for orbit removal of spent launchers' stages. *Acta Astronaut.* **2016**, *119*, 118–130, doi:10.1016/j.actaastro.2015.11.012.
7. Benvenuto, R.; Lavagna, M.; Salvi, S. Multibody dynamics driving GNC and system design in tethered nets for active debris removal. *Adv. Sp. Res.* **2016**, *58*, 45–63, doi:10.1016/j.asr.2016.04.015.
8. Botta, E.M.; Miles, C.; Sharf, I. Simulation and tension control of a tether-actuated closing mechanism for net-based capture of space debris. *Acta Astronaut.* **2020**, *174*, 347–358, doi:10.1016/j.actaastro.2020.04.052.
9. Dudziak, R.; Tuttle, S.; Barraclough, S. Harpoon technology development for the active removal of space debris. *Adv. Sp. Res.* **2015**, *56*, 509–527, doi:10.1016/j.asr.2015.04.012.
10. Aslanov, V.; Yudintsev, V. Dynamics of large space debris removal using tethered space tug. *Acta Astronaut.* **2013**, *91*, 149–156, doi:10.1016/J.ACTAASTRO.2013.05.020.
11. Zhang, J.; Ye, D.; Biggs, J.D.; Sun, Z. Finite-time relative orbit-attitude tracking control for multi-spacecraft with collision avoidance and changing network topologies. *Adv. Sp. Res.* **2019**, *63*, 1161–1175, doi:10.1016/j.asr.2018.10.037.
12. Zhang, J.; Biggs, J.D.; Ye, D.; Sun, Z. Extended-State-Observer-Based Event-Triggered Orbit-Attitude Tracking for Low-Thrust Spacecraft. *IEEE Trans. Aerosp. Electron. Syst.* **2020**, *56*, 2872–2883, doi:10.1109/TAES.2019.2955257.
13. Zhang, J.; Biggs, J.D.; Ye, D.; Sun, Z. Finite-time attitude set-point tracking for thrust-vectoring spacecraft rendezvous. *Aerosp. Sci. Technol.* **2020**, *96*, 105588, doi:10.1016/j.ast.2019.105588.
14. Hartley, E.N.; Trodden, P.A.; Richards, A.G.; Maciejowski, J.M. Model predictive control system design and implementation for spacecraft rendezvous. *Control Eng. Pract.* **2012**, *20*, 695–713, doi:10.1016/j.conengprac.2012.03.009.
15. Breger, L.S.; How, J.P. Safe Trajectories for Autonomous Rendezvous of Spacecraft. *J. Guid. Control. Dyn.* **2008**, *31*, 1478–1489, doi:10.2514/1.29590.
16. Liu, X.; Lu, P. Solving Nonconvex Optimal Control Problems by Convex Optimization. *J. Guid. Control. Dyn.* **2014**, *37*, 750–765, doi:10.2514/1.62110.
17. Lu, P.; Liu, X. Autonomous Trajectory Planning for Rendezvous and Proximity Operations by Conic Optimization. *J. Guid. Control. Dyn.* **2013**, *36*, 375–389, doi:10.2514/1.58436.
18. Ventura, J.; Ciarcià, M.; Romano, M.; Walter, U. Fast and Near-Optimal Guidance for Docking to Uncontrolled Spacecraft. *J. Guid. Control. Dyn.* **2016**, 1–17, doi:10.2514/1.G001843.
19. Sabatini, M.; Palmerini, G.B.; Gasbarri, P. A testbed for visual based navigation and control during space rendezvous operations. *Acta Astronaut.* **2015**, *117*, 184–196, doi:10.1016/j.actaastro.2015.07.026.
20. Ivanov, D.; Koptev, M.; Ovchinnikov, M.; Tkachev, S.; Proshunin, N.; Shachkov, M. Flexible microsatellite mock-up docking with non-cooperative target on planar air bearing test bed. *Acta Astronaut.* **2018**, *153*, 357–366, doi:10.1016/j.actaastro.2018.01.054.
21. Cloutier, J.R.; Stansbery, D.T. The capabilities and art of state-dependent Riccati equation-based design. In Proceedings of the Proceedings of the 2002 American Control Conference (IEEE Cat. No.CH37301); American Automatic Control Council; Vol. 1, pp. 86–91.
22. Cloutier, J.R.; Cockburn, J.C. The state-dependent nonlinear regulator with state constraints. *Proc. Am. Control Conf.* **2001**, *1*, 390–395, doi:10.1109/ACC.2001.945577.
23. Çimen, T. Survey of State-Dependent Riccati Equation in Nonlinear Optimal Feedback Control Synthesis. *J. Guid. Control. Dyn.* **2012**, *35*, 1025–1047, doi:10.2514/1.55821.
24. Navabi, M.; Reza Akhloumadi, M. Nonlinear Optimal Control of Orbital Rendezvous Problem for Circular and Elliptical Target Orbit. *Modares Mech. Eng.* **2016**, *15*, 132–142.
25. Felicetti, L.; Palmerini, G.B. A comparison among classical and SDRE techniques in formation flying orbital control. In Proceedings of the IEEE Aerospace Conference Proceedings; 2013.
26. Stansbery, D.T.; Cloutier, J.R. Position and attitude control of a spacecraft using the state-dependent Riccati equation technique. *Proc. Am. Control Conf.* **2000**, *3*, 1867–1871, doi:10.1109/acc.2000.879525.
27. Segal, S.; Gurfil, P. Effect of Kinematic Rotation-Translation Coupling on Relative Spacecraft Translational Dynamics. *J. Guid. Control. Dyn.* **2009**, *32*, 1045–1050, doi:10.2514/1.39320.
28. Lee, D.; Bang, H.; Butcher, E.A.; Sanyal, A.K. Kinematically Coupled Relative Spacecraft Motion Control Using the State-Dependent Riccati Equation Method. *J. Aerosp. Eng.* **2015**, *28*, 04014099, doi:10.1061/(ASCE)AS.1943-5525.0000436.
29. Akhloumadi, M.; Ivanov, D. Influence of Satellite Motion Control System Parameters on Performance of Space Debris Capturing. *Aerosp. 2020, Vol. 7, Page 160* **2020**, *7*, 160, doi:10.3390/AEROSPACE7110160.